

Aromaticity and Electron Affinity of Carbo^k-[3]radialenes, $k = 0, 1, 2$

Christine Lepetit,^[a] Mogens Brøndsted Nielsen,^[b] François Diederich,^[c] and Remi Chauvin^{*[a]}

Abstract: Aromaticity enhancement is a possible driving force for the low reduction potentials of buta-1,3-diyne-diyli-expanded $[N]$ radialenes: this hypothesis is theoretically analyzed for the expanded [3]radialene prototype. This study is undertaken within a more general prospect, namely the evaluation of the variation of aromaticity with endocyclic and peripheral carbomeric expansion of [3]radialene and its mono- and dianions. The structures, denoted as $[C-H]_6^h[C-C]_3^k$ carbo-[3]radialene(q) ($h = 0, 1; k = 0, 1, 2; q = 0, -1, -2$), were optimized in relevant singlet, doublet, or triplet spin states at the B3PW91/6-31G** level. They were found to be all planar. The structural aromaticity was measured through the average bond length d_{av} over the $[C-C]_3^k$ carbo-[3]radialene core, and by the corresponding bond-length equalization parameter $\sigma(d)$, related to Krygowski's GEO. The magnetic aromaticity was measured by Schleyer's NICS values at the center of the rings. Regarding the relative varia-

tion of NICS and $\sigma(d)$, two classes of species can be distinguished according to their endocyclic expansion level. The species with a nonexpanded ($k=0$) or doubly expanded ($k=2$) ring constitute the first class: they exhibit D_{3h} symmetry and a strong correlation of NICS with $\sigma(d)$. The species with a singly expanded ring ($k=1$) fall far from the correlation line, and constitute the second class. This class distinction is related to the degeneracy scheme of the frontier orbitals of the neutral representative. A finer appraisal of the electron (de)localization is brought by the ELF (Electron Localization Function) analysis of the electron density. It allows for a weighting of relevant resonance forms. Unsubstituted species are well described by the superimposition of two or three resonance

forms. For (doublet spin state) mono-anionic species, their respective weights are validated by comparison with AIM spin density. The weighted mean, n , of the formal numbers of paired π_z electrons in the resonance forms was calculated and compared with the closest even integer of either forms $4m+2$ or $4m$. A density-based continuous generalization of the orbital-based discrete Hückel rule is then heuristically proposed through an analytical correlation of NICS versus $\sigma(d)$, n , and S , the spin of the species. The frontier-orbital-degeneracy pattern of neutral species is discussed with respect to structural and magnetic aromaticity criteria. A decreasing HOMO–LUMO gap versus endocyclic expansion is obtained, but $[C-C]_3^1$ carbo-[3]radialene possesses the highest HOMO and LUMO energies. Vertical and adiabatic electron affinities of neutral and monoanionic species were also computed and compared with related experimental data.

Keywords: aromaticity • conjugation • ELF (Electron Localization Function) • expanded radialenes • redox chemistry

Introduction

Planar radialenes (C_2H_2) _{N} exhibit essential common features of and differences from planar annulenes (CH) _{N} : they both contain a cyclic sequence of N conjugated sp^2 carbon atoms,

but while the double bonds of radialenes are cross-conjugated, those of annulenes are linearly conjugated. Nevertheless, the question of aromaticity addresses both classes. While annulenes are markedly differentiated as aromatic or anti-aromatic, radialenes, owing to their poor stability in their unsubstituted version, have long been considered as non-aromatic additive assemblies of vinylidene units.^[1] Expansion of annulenes^[2, 3] and radialenes^[4] by inserting one or two $sp-C_2$ units into all bonds of the rings results in an extension of the conjugation of out-of-plane π_z MOs (and in the appearance of homoconjugated in-plane π_{xy} MOs) in the corresponding ring “carbomers”.^[5] The consequences on aromaticity deserve a comparative study. It is worth remembering here that expansion of cycloalkanes leads to $[N]$ pericyclines,^[6] and the question of their homoaromaticity has already been addressed.^[7] In the case of $[N]$ annulenes, it has been theoretically shown that their aromaticity is definitely pre-

[a] Prof. R. Chauvin, Dr. C. Lepetit
Laboratoire de Chimie de Coordination, UPR 8241 CNRS
205 Route de Narbonne, 31077 Toulouse Cedex 4 (France)
Fax: (+33)5-61-55-30-03
E-mail: chauvin@lcc-toulouse.fr

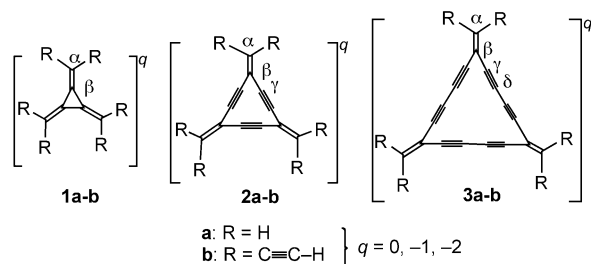
[b] Dr. M. Brøndsted Nielsen
Department of Chemistry, University of Southern Denmark
Campusvej 55, 5230 Odense M (Denmark)

[c] Prof. F. Diederich
Laboratorium für Organische Chemie, ETH-Hönggerberg
HCI, 8093 Zürich (Switzerland)

Supporting information for this article is available on the WWW under <http://www.chemeurj.org> or from the author.

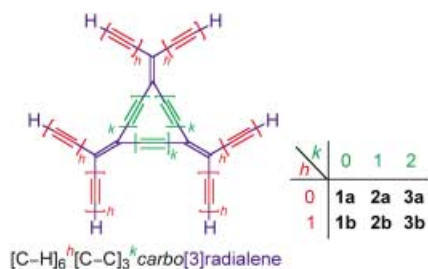
served in the corresponding carbo- $[N]$ annulenes.^[8] The case of radialenes is a priori more challenging: does the expansion effect overcome the topological effect, and bring some aromatic character to the corresponding carbo- $[N]$ radialenes? The question is hereafter addressed for the parent [3]radialene prototype, an isomer of benzene.

Several derivatives of [3]radialene **1a** (Scheme 1) have been experimentally described,^[9] and very recent thermochemical calculations have suggested that **1a** might be slightly



Scheme 1. Eighteen carbo-[3]radialenic species investigated in this study. $q = 0$: neutral, $q = -1$: monoanion, $q = -2$: dianion.

aromatic in the energetic sense.^[10] Additional data on the aromatic status of **1a** itself are thus still desirable. Moreover, aromaticity enhancement might be an explanation for the remarkably facile reduction experienced by a perethynylated [3]radialene, a silylated derivative of **1b**.^[11] Indeed, according to cyclic voltammetry, this radialene was able to accommodate two electrons in two distinct one-electron reduction steps (vide infra). Moreover, perethynylated buta-1,3-diyne-expanded (doubly expanded) [3]- and [4]radialenes were readily reduced electrochemically.^[4c-e] In order to explain these experimental observations and thereby possibly extend the Hückel rule to cross-conjugated rings, we decided to carry out a detailed theoretical study on [3]radialenes, varying the parent structure with respect to: i) the expansion level of endocyclic C–C bonds, k , and/or peripheral C–H bonds, h , and ii) the reduction level, q ($q = 0$: neutral, $q = -1$: monoanion, $q = -2$: dianion). A set of eighteen species denoted as $[\mathbf{na}]^q$ or $[\mathbf{nb}]^q$ is considered ($\mathbf{n} = 1-3$). According to a previously proposed nomenclature, their generic name is: $[\text{C-H}]_6^h[\text{C-C}]_3^k\text{carbo}[3]\text{radialene}(q)$ ($q = 0, -1, -2$; $k = 0, 1, 2$; $\mathbf{a}: h = 0, \mathbf{b}: h = 1$) (Schemes 1 and 2).



Scheme 2. Carbomeric expansion of endocyclic C–C and/or peripheral C–H bonds in a [3]radialene. $k = 0$: parent radialene, $k = 1$: ethynediyl-expanded radialene, $k = 2$: buta-1,3-diyne-expanded radialene. $h = 0$: unsubstituted radialene, $h = 1$: ethynyl-substituted radialene.

The goal is threefold.

- 1) *Compare* the aromaticity of **1a–3a** and **1b–3b** and the corresponding mono- and dianions on the basis of structural (bond length equalization, $\sigma(d)$, and average bond length, d_{av}) and magnetic (Nucleus Independent Chemical Shift, NICS) criteria.^[12]
- 2) *Quantify* the electronic delocalization from electron localization function (ELF) analysis,^[13] and translate the results in terms of weighted resonance structures through a recently disclosed method based on the integration of electron density over ELF basins.^[7d]
- 3) *Analyze* the orbital diagrams, the chromophore properties (HOMO–LUMO gap), and the redox properties (electron affinities, EA) of related species.

Computational Methods

Calculations of structure and properties of neutral and anionic species were performed at the DFT level by using the B3PW91 functional. It is indeed now recognized that despite the existence of occupied MOs with positive eigenvalues, the DFT method is reliable for predicting properties of negatively charged species, and especially of carbon-rich molecules such as linear carbon chains HC_nH .^[14]

Geometries were thus fully optimized at the B3PW91/6-31G** level by using Gaussian98.^[15] Vibrational analysis was performed at the same level in order to check that a minimum on the potential energy surface was obtained.

NICS values were computed at the B3PW91/6-31 + G** level according to the procedure described by Schleyer et al.^[16] The magnetic shielding tensor was calculated for a ghost atom located at the center of the ring by using the GIAO (gauge-including atomic orbital)^[17] method implemented in Gaussian98. For small rings, NICS at 0.6 Å above the ring center was shown to minimize the paratropic contribution of the proximate σ bonds. For a comparative purpose, however, the fixation of a nonzero height parameter over a large range of ring sizes (3–15 atoms) would be quite arbitrary in the present case. Keeping in mind that Shaik and Hiberty showed that the electronic delocalization of benzene is imposed by σ bonds,^[18] NICS values have been calculated at the center of gravity of either small or large rings. They *globally* measure the magnetic effect of the delocalization of σ and π electrons, naturally weighted by their respective distance to the ring center, without *analytical* separation in diatropic/paratropic effects.

ELF topological analysis was carried out with TopMoD.^[19] Visualization of ELF isosurfaces and basins was done with the freeware SciAn.^[20]

Atomic charges and spin densities were derived from atoms-in-molecules (AIM) analysis,^[21] by using TopMoD.^[19]

Results and Discussion

Structural and magnetic aromaticity criteria

Effect of ring expansion: The geometry of \mathbf{na} and $[\mathbf{na}]^-$ was calculated in the singlet and doublet spin states, respectively. The geometry of $[\mathbf{na}]^{2-}$ was calculated in the singlet or triplet spin state. The results are listed in Table 1.

The optimized structure of [3]radialene **1a** is similar to that of various derivatives as determined by X-ray crystallography,^[11, 22] and to recent calculations at the B3LYP/6-311G(d,p) level.^[23] All the $[\mathbf{na}]^q$ structures were found to be planar. Their symmetry is D_{3h} except for $[\mathbf{2a}]^-$, which exhibits C_{2v} symmetry. The singlet state of $[\mathbf{2a}]^{2-}$ exhibits C_s symmetry with two planar $=\text{CH}_2$ units and one pyramidalized $-\text{CH}_2^-$ unit. The

Table 1. NICS values and geometric parameters of nine $[C-C]_3^k$ carbo-[3]radialenic species.^[a]

	Symmetry	Bond lengths [Å]			d_{av} [Å] ^[b]	$\sigma(d)$ [Å] ^[c]	NICS [ppm]
		<i>exo</i> -C=CH ₂	<i>endo</i> -Csp ² -C	<i>endo</i> -C≡C			
1a	<i>D</i> _{3h}	1.334	1.442		1.389	0.054	-11.4
	=	+	-		+	-	-
[1a] ^{-[d]}	<i>D</i> _{3h}	1.366	1.418		1.392	0.026	-24.5
	=	+	-		+	-	-
[1a] ^{2-[e]}	<i>D</i> _{3h}	1.400	1.406		1.403	0.006	-31.2
2a	<i>D</i> _{3h}	1.345	1.438	1.223	1.361	0.088	-7.0
	=	+	-	+	+	-	+
[2a] ⁻	<i>C</i> _{2v}	1.352	1.404 × 2	1.246	1.366	0.080	+4.0
		1.387 × 2	1.437 × 2	1.230 × 2			
			1.439 × 2				
	+	+	-	+	+	+	-
[2a] ²⁻ triplet	<i>D</i> _{3h}	1.404	1.422	1.245	1.373	0.084	-15.0
3a	<i>D</i> _{3h}	1.351	1.431	1.223	1.336	0.086	+1.5
	=	+	-	+	+	-	-
[3a] ⁻	<i>D</i> _{3h}	1.371	1.422	1.231	1.338	0.080	-2.2
	=	+	-	+	+	-	+
[3a] ²⁻	<i>D</i> _{3h}	1.390	1.418	1.240	1.342	0.076	-3.7

[a] Optimized geometries were obtained for singlet spin state at the B3PW91/6-31G** level, unless otherwise mentioned NICS values were computed at the B3PW91/6-31 + G** level. The +/− signs underline the sense of variation of column quantities from the top line to the bottom line. [b] Average C–C bond length. [c] $\sigma(d) = (1/N \sum (d_i - d_{av})^2)^{1/2}$ in which N is the number of C–C bonds (6, 12, or 15). [d] At the B3PW91-6-311 + G** level. [e] At the B3PW91-6-31 + G** level.

triplet state of [**2a**]²⁻, however, is more stable by 14 kcal mol⁻¹ and has *D*_{3h} symmetry.

It is remarkable that whatever the structure [**na**]^q, the length of each bond type varies in the same manner upon reduction to [**na**]^{q-1}: the length of short bonds increases while the length of long bonds decreases (Table 1). Reduction thus results in an average bond length equalization and thus to the enhancement of the overall (*exo* + *endo*, π + σ) electron delocalization. The delocalization is structurally measured by $\sigma(d)$, namely the root mean square deviation from the overall average C–C bond length, d_{av} , over the radiacycle.^[24] The effect of reduction on overall delocalization is thus quantified by the $\sigma(d)$ variation, which is negative for all structures but [**2a**]⁻. The additional electron is thus localized over single bonds and attracts electron density from multiple bonds. This observation may be related to a spin-pairing effect, and calls for the use of a suited analytical tool, namely the ELF analysis (*vide infra*).^[13]

It is worth noting that the mean bond length, d_{av} , of any structure increases slightly, but systematically, upon reduction. This indicates that, despite an enhanced delocalization, the carbon atoms are globally less tightened after reduction. $\sigma(d)$ and d_{av} are directly related to Krygowski's geometric (GEO) and energetic (EN) structural aromaticity parameters, respectively.^[24] Their inverse variation with reduction illustrates the difference between geometric and energetic aromaticity (*vide infra*).

All the species [**na**]^q, except [**2a**]⁻, have a negative NICS value at the center of the ring, and can be considered to be magnetically aromatic.^[16] For neutral species, the NICS value of a (expanded) cyclotrisvinylidene (radialene) can be compared with that of the (expanded) cyclotrisvinylene (annulene) isomer with at least the same symmetry. At a similar level of theory, one gets: NICS(**1a**) = -11.4 ppm versus NICS(*D*_{6h} benzene) = -8.0 ppm;^[8b-c] NICS(**2a**) = -7.0 ppm

versus NICS(*D*_{3h} hexadehydro[12]annulene) = +106.1 ppm (“abnormal” value discussed in ref. [25]); NICS(**3a**) = +1.5 ppm versus NICS(*D*_{3h} dodecadehydro[18]annulene) = -10.4 ppm,^[25] and NICS(*D*_{6h} [C–C]₆carbobenzene) = -17.9 ppm.^[8b-c] According to the NICS(0) criterion, **1a** and **2a** are thus more magnetically aromatic than their isomers, but the converse holds for **3a**.

On the basis of the NICS variation, [**1a**]^q and [**3a**]^q experience an enhancement of magnetic aromaticity upon reduction. A similar trend was reported for the double deprotonation of deltic acid to the oxocarbon dianion (CO)₃²⁻ (Δ NICS(0) = -2.1 ppm, HF/6-311 + G**).^[26a] The one-electron reduction of the magnetically aromatic expanded radialene **2a** yields a magnetically antiaromatic anion [**2a**]⁻ (NICS = +4 ppm). “Normal” behavior is, however, restored when considering the two-electron reduction of **2a** to the magnetically aromatic triplet dianion [**2a**]²⁻. From Table 1, magnetic aromaticity (NICS) and geometric aromaticity ($\sigma(d)$) vary in the same sense in the [**1a**]^q and [**3a**]^q series, but vary in the opposite sense in the [**2a**]^q series. The consistency between magnetic aromaticity and geometric aromaticity thus deserves to be scrutinized (*vide infra*).

Effect of substitution: The effect of substitution (expansion of the C–H bonds) of **1a**–**3a** by six ethynyl units was envisioned. The C≡C–Ar substituents of experimental structures were simplified for C≡C–H.^[4d,e] The geometry of **1b**, **2b**, **3b** and their mono- and dianions were calculated at the same level as above.

The results show that substitution does not qualitatively affect the trends established in the unsubstituted series **1a**–**3a** (Table 2 versus Table 1): the optimized symmetry of [**nb**]^q is identical to that of [**na**]^q, except for dianions [**1b**]²⁻ and [**2b**]²⁻, which exhibit a slight distortion of the C≡C–H bond angles. The bond lengths and bond angles of the [C–C]₃^kcarbo-

Table 2. NICS(0) and geometric parameters of the nine hexaethynyl-[C-C]₃^kcarbo-[3]radialenic species.^[a]

	Symmetry	Bond lengths [Å]						d_{av} [Å]	$\sigma(d)$ [Å]	NICS [ppm] ^[b]
		<i>exo</i> -C=C	<i>endo</i> -Csp ² -C	<i>endo</i> -C≡C	<i>endo</i> -C-C	<i>exo</i> -Csp ² -C	<i>exo</i> -C≡C			
1b	<i>D</i> _{3h}	1.369	1.417			1.421	1.212	1.389	0.029	-22.7
	=	+				-	+	+	-	-
[1b]⁻	<i>C</i> ₁	1.390	1.406			1.419	1.216	1.398	0.008	-26.4
	=	+	-			-	+	+	-	-
[1b]²⁻	<i>D</i> _{3h}	1.415	1.398			1.413	1.226	1.403	0.003	-27.1
2b	<i>D</i> _{3h}	1.379	1.423	1.226		1.419	1.211	1.363	0.081	-7.1
	=	+	-	+		-	+	+	-	-
[2b]⁻	<i>C</i> ₁	1.424	1.437 × 2	1.224		1.411 × 2	1.218 × 2	1.367	0.078	-16.4
	=	1.393 × 2	1.402 × 2	1.239 × 2		1.419 × 2	1.214 × 4			
			1.405 × 2			1.418 × 2				
	+	+	-	+		-	+	+	+	-
[2b]²⁻	<i>D</i> _{3h}	1.429	1.409	1.240		1.411	1.222	1.372	0.077	-14.6
3b	<i>D</i> _{3h}	1.386	1.416	1.226	1.352	1.418	1.212	1.337	0.081	-1.2
	=	+	-	+	-	-	+	+	-	-
[3b]⁻	<i>D</i> _{3h}	1.407	1.408	1.232	1.346	1.415	1.215	1.339	0.078	-2.3
	=	+	-	+	-	-	+	+	-	-
[3b]²⁻	<i>D</i> _{3h}	1.424	1.403	1.238	1.342	1.413	1.219	1.341	0.074	-4.6

[a] Geometry optimizations were carried out at the B3PW91/6-31G** level. NICS values were computed at the B3PW91/6-31 + G** level. The +/− signs underline the sense of variation of column quantities from the top line to the bottom line. [b] d_{av} and $\sigma(d)$ do not explicitly take into account the ethynyl substituents, and are calculated over the [C-C]₃^kcarbo-[3]radialenic core.

[3]radialenic core are similar to those of the unsubstituted series. In Table 2, the variation of the vertical entries upon reduction is always in the same sense as in Table 1.

The bond-length-equalization parameter limited to the [C-C]₃^kcarbo-[3]radialenic core of [nb]^q, $\sigma(d)$, is systematically slightly shorter than that of the corresponding unsubstituted structure [na]^q. Likewise, the NICS value of [nb]^q is always smaller than that of the corresponding [na]^q structure. Ethynyl substitution thus induces a consistent enhancement of (cyclic) delocalization over the [C-C]₃^kcarbo[3]radialenic core. Nevertheless, a dramatic effect of substitution is observed for the antiaromatic anion [2a]⁻ (NICS = +4 ppm), which gives the strongly aromatic anion [2b]⁻ (NICS = -16.4 ppm).

Correlation of magnetic aromaticity with structural aromaticity: In both the nonexpanded (**1**) and doubly expanded (**3**) series, the stronger the bond length equalization, the more negative the NICS value (Figure 1). For ten of the species [nx]^q ($n = 1, 3$) an exceptional linear correlation is obtained:

$$\text{NICS} = -34.15 + 405.5 \sigma(d), R = 0.9986 \quad (1)$$

This shows that geometric and magnetic aromaticity criteria vary in a highly parallel manner in series **1** and **3**. The monoexpanded species [2a]^q and [2b]^q, however, do not fit into the correlation. For **2a** → [2a]⁻, the magnetic dearomatization ($\Delta\text{NICS} > 0$) is consistent with group desymmetrization ($D_{3h} \rightarrow C_{2v}$), but a priori not with bond-length equalization ($\Delta\sigma(d) < 0$). Conversely, for [2a]⁻ → [2a]²⁻, the magnetic aromatization ($\Delta\text{NICS} < 0$) is consistent with group symmetrization ($C_{2v} \rightarrow D_{3h}$), but a priori not with bond-length differentiation ($\Delta\sigma(d) > 0$). A similar situation was reported by Krygowski for radialene,^[6] which was found to be magnetically antiaromatic (NICS = +2.8 ppm), but exhibits a perfect bond-length equalization ($\text{GEO} = \alpha\sigma^2(d) = 0$: C=CH₂ and C-C bonds have equal lengths!).^[27] The GEO parameter,

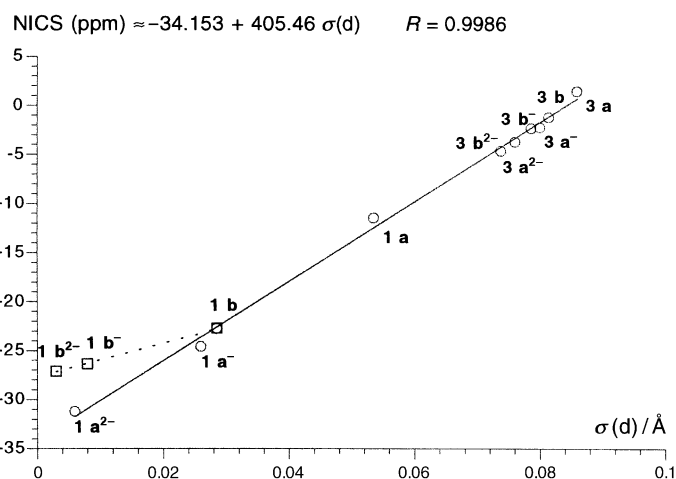


Figure 1. Correlation of NICS versus $\sigma(d)$ for species [na]^q and [nb]^q with nonexpanded and doubly expanded rings ($n = 1, 3$). [1b]⁻ and [1b]²⁻ (□) were not included in the linear regression, but even for these species, the agreement is qualitatively acceptable (ca. 17% error). Moreover, the three [1b]^q species ($q = 0, -1, -2$) are perfectly aligned.

and thus $\sigma(d)$, is not sufficient for ranking structural aromaticity (e.g., $\sigma(d)$ vanishes for all symmetric structures such as benzene or the cyclopropenium cation). An additional EN parameter was thus defined to evaluate the discrepancy between d_{av} and d_{opt} , where the bond length is in a perfectly C-C ↔ C=C resonating system.^[24] The evaluation of the d_{opt} parameter for mixed systems involving both sp²- and sp-hybridized atoms would require a full study, which is outside the scope of this report.^[28] Nevertheless, plotting NICS versus d_{av} over the homogeneous set of NICS-negative [nx]^q species affords a qualitatively good correlation ($R = 0.98$, except for **1a**), including the monoexpanded series [2a]^q and [2b]^q (Figure 2).

The magnetically antiaromatic anion [2a]⁻ should deserve a separate treatment.

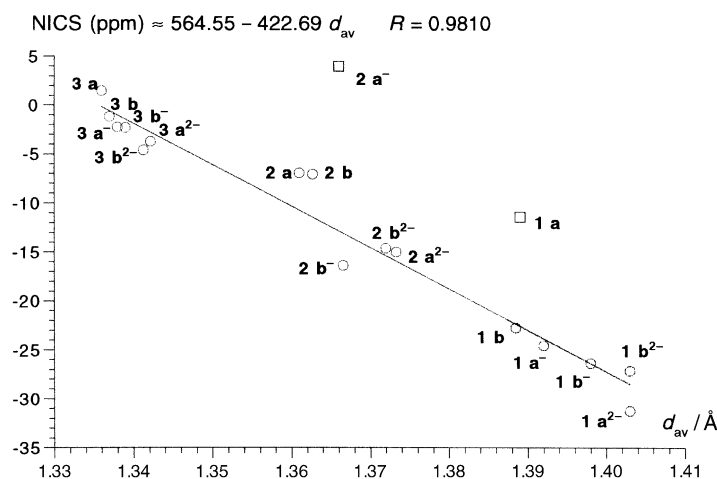


Figure 2. Correlation of NICS versus d_{av} , the mean bond lengths over the $[C-C]_3^k$ carbo-[3]radialenic core for species $[na]^q$ and $[nb]^q$. The correlation extends to all compounds except the parent radialene **1a** and the magnetically antiaromatic anion $[2a]^-$ (\square).

The negative slope of the regression line means that the more magnetically aromatic the species, the less stabilizing the structure with respect to dissociation. The apparent orthogonality of magnetic and energetic aromaticities,^[29] may exemplify Katritzky's factor analysis and suggests that "aromaticity" is a two-dimensional concept.^[30] Nevertheless, while the NICS value depends on the ring current, and thus on the endocyclic electron delocalization, d_{av} takes into account both endocyclic and radial electron delocalization. Therefore, NICS was plotted against d'_{av} , the average bond length over the ring only. This however afforded a much less accurate correlation ($NICS \sim 382 - 289 d'_{av}$, $R' = 0.926 \ll 0.980$), and the slope, if meaningful, though still negative, is divided by 1.5. This shows that the *exocyclic double bonds are explicitly involved in the aromatic system*.

Finally, according to NICS, $\sigma(d)$, and d_{av} measures, magnetic aromaticity varies as geometric aromaticity, but not as energetic aromaticity.

ELF analysis:^[13, 31] After having considered the *effects* of "cyclic" electron delocalization, we now consider the electron delocalization *itself*, using the ELF analysis of the electron density.

Topological analysis of the ELF gradient field yields a partition of the molecular position space into basins of attractors (i.e. the local maxima of ELF) bearing a chemical meaning.^[13, 32] These basins closely match the electronic domains defined by Gillespie in the VSEPR model, and therefore ELF analysis provides a reliable mathematical sophistication of Lewis' valence and Gillespie's

VSEPR models. The ELF basins are classified as core, valence bonding, and nonbonding basins. A core basin contains a nucleus X (except a proton) and will be referred to as C(X). A valence bonding basin lies between two or more core basins. Each valence bonding basin is characterized by its synaptic order, which is the number of core basins with which it shares a common boundary. The monosynaptic basins therefore correspond to nonbonded pairs (referred to as V(X)) whereas the di- and polysynaptic ones are related to bi- or multicentric bonds (referred to as V(X₁, X₂, X₃, ...)). The average populations of the basins may be obtained by integration of the electron density. They are not expected to have integral values, but the bond populations were found to be roughly equal to twice the topologically defined Lewis bond orders in extensive studies of chemical bonding.

Qualitative analysis of the ELF populations: The ELF analysis was performed for $[1a]^q$, $[2a]^q$, $[3a]^q$, $q = 0, -1$, and $[3a]^{2-}$. For neutral species **1a–3a**, the ELF populations are in agreement, with the "natural" Lewis structure as the dominant resonance form. In all cases, however, single-bond basins contain slightly more than two electrons: 2.1 for Csp²–Csp², 2.3 for Csp²–Csp basins, and 2.6 for Csp–Csp basins. Conversely, multiple-bond basins contain slightly less the theoretical number of electrons: 3.5 for Csp²=Csp² and 5.3 for Csp=Csp (Figure 3). This indicates that some delocalization occurs in all the neutral structures.

After reduction, the additional electron does not localize into a monosynaptic valence basin but rather scatters into the pre-existing disynaptic valence basins. In the [3]radialene anion $[1a]^-$, the localization of the additional electron is mainly endocyclic, while for the monoexpanded anion, $[2a]^-$, it is mainly exocyclic. In the doubly expanded anion, $[3a]^-$, the additional electron is equally shared between exocyclic and endocyclic basins. Therefore, the additional electron of reduced species is absorbed by the ring in $[1a]^-$ and $[3a]^-$ and is repelled to the peripheral *exo* bonds in $[2a]^-$. As far as

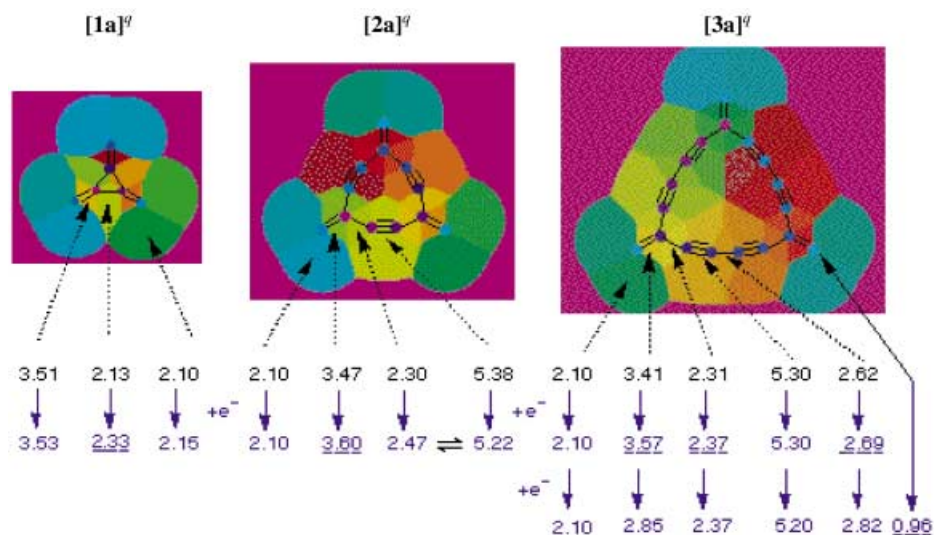


Figure 3. ELF basins of unsubstituted carbo-[3]radialenic species, and variation of their respective populations upon reductions. Underlined populations correspond to the main localization of the additional electron(s) with respect to the neutral form. The values of the ELF populations given for the C_{2v}-symmetric anion $[2a]^-$ are averaged in the D_{3h} approximation.

aromaticity is related to the *endocyclic* electron delocalization, these results are consistent with the decrease of magnetic and structural aromaticity during the first reduction of **2a** (notice that despite the exact C_{2v} symmetry of $[2a]^-$, the values of the ELF populations given in Figure 3 are averaged in the D_{3h} approximation). The ELF analysis of the electron density (Figure 3) is in qualitative agreement with the structural effect on the bond-length equalization (Table 1).

After the second reduction, the dianion of the doubly expanded[3]radialene, $[3a]^{2-}$, exhibited a monosynaptic valence basin at the CH_2 termini. It corresponds to the lone pair of a localized carbanion. The electron density of the adjacent *exo* double bonds of the intermediate monoanion $[3a]^-$ was equally shared between the lone pair basins and the ring basins. The second reduction process thus results in a localization of the electron density at the periphery of $[3a]^{2-}$.

Quantification of resonance forms: Resonance theory, or mesomerism, is convenient for the visualization of aromaticity: the cyclic delocalization of π electrons is measured by the degree of equivalence of Kekulé-like resonance forms. Relevant resonance forms are Lewis structures, whose stability is selected on the basis of classical rules.^[33] Quantitative weighting of resonance forms has been attempted by different methods.^[7d, 12a, 24, 34] A method based on ELF analysis has recently been disclosed,^[7d] and is applied here to the neutral and anionic unsubstituted $[na]^q$, $q = 0, -1$. The most relevant resonance forms have been selected according to classical rules,^[33] and upon consideration of AIM charges and spin densities. A system of linear equations relating the ELF basins populations and bond orders of the weighted Lewis structures may then be written. The least-squares method is applied to solve the linear equations system when no exact solution is available. The procedure is illustrated in the Supporting Information for the case of $[3a]^{2-}$ (see below).

The results are summarized in Figure 4. The six compounds are well described by two, or at most three, types of nonequivalent resonance forms.

The major form (60%) of [3]radialene **1a** is nonzwitterionic, and has a greater weight than all the minor zwitterionic forms ($6 \times 6.7 = 40\%$). This, however, indicates that electron delocalization occurs in [3]radialene. This is consistent with the very negative NICS value and with recent thermochemical estimates, by aromatic stabilization energies (ASE), of the energetic aromaticity of [3]radialene.^[10] In the reduced species $[1a]^-$, two types of resonance forms occur: the weight of three equivalent forms ($3 \times 11.3 = 34\%$) is almost equal to the weight of six other equivalent forms ($6 \times 11.0 = 66\%$). This indicates an enhanced electron delocalization. In accordance with the higher stability of secondary carbanions, the negative charge remains at the exocyclic carbons Ca rather than at the endocyclic ones, $C\beta$ (see Scheme 1). This resonance weighting is in perfect accordance with the calculated AIM spin density: 66% at Ca and 34% at $C\beta$ (see Supporting Information).

The major (or minor) resonance form of **2a** is the ring carbomer of the major (or minor) form of **1a**, and the corresponding weights are preserved. This is a quantitative illustration of the statement that resonance is preserved by

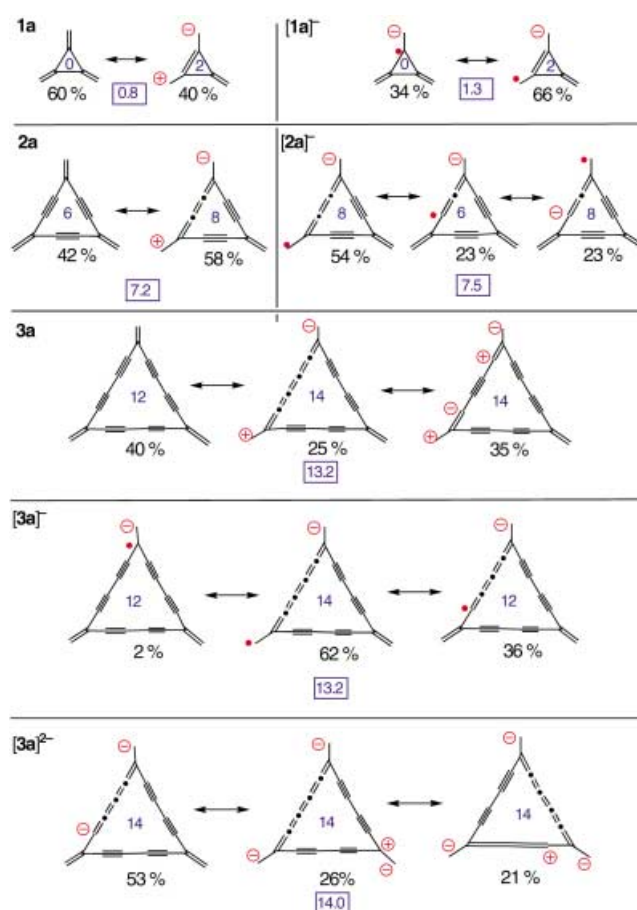
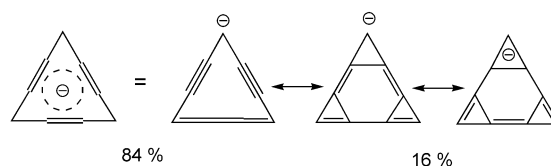


Figure 4. ELF-based quantification of resonance forms of $[na]^q$ species. The formal number (n) of paired π_e electrons inside the ring and their weighted mean are given in the square cells.

“carbomerization”.^[5] Attempts to consider mesomeric forms featuring possible in-plane homoaromaticity (Dewar-type valence isomers with three additional σ bonds) yields negligible weights for the corresponding Lewis structures. This situation is markedly different from that of $[C_3C_3]$ carbocyclopropenyliide, in which in-plane homoaromaticity was evidenced through a nonzero weight (16%) of the corresponding σ resonance forms (Scheme 3).^[7d]



Scheme 3. Resonance weighting of $[C-C]_3$ carbocyclopropenyliide ion.^[7d]

The major resonance forms of the reduced species $[2a]^-$ exhibit a maximum separation of formal atomic spin and atomic charge.^[35] These forms occur with about the same weight as their carbomeric resonance forms in $[1a]^-$ (54% versus 66%). Nevertheless, in $[2a]^-$, the resonance forms with adjacent atomic spin and charge ($[1a]^-$: $3 \times 11.3 = 34\%$) are negligible. Instead, spin and charge undergo an intermediate separation at Ca and $C\gamma$ ($2 \times 6 \times 3.8 = 2 \times 23 = 46\%$). This

resonance weighting is again in accordance with the calculated AIM spin density: AIM($C\alpha$) = 80% (ELF resonance: 77%), AIM($C\beta$) = 0% (ELF resonance: 0%), AIM($C\gamma$) = 20% (ELF resonance: 23%) (see Supporting Information). According to this analysis, the radical is absent from the $C\beta$ vertices. This suggests a limited cyclic delocalization and thus a reduced aromaticity, in agreement with the positive NICS value for $[2\mathbf{a}]^-$.

The major form (40%) of $3\mathbf{a}$ is the second-generation ring carbomer of the major form (60%) of $1\mathbf{a}$. The minor zwitterionic form ($6 \times 4.2 = 25\%$) of $3\mathbf{a}$ is the second-generation ring carbomer of the minor forms ($6 \times 6.7 = 40\%$) of $1\mathbf{a}$. Other forms are required to obtain a resolvable system of equation. These forms ($6 \times 5.8 = 35\%$) contain an alternating double $+/-$ charge separation. As in $[2\mathbf{a}]^-$, the major resonance forms of the reduced species $[3\mathbf{a}]^-$ exhibit a maximal separation of spin and charge, and occur with about the same weight as their carbomeric resonance forms in $[1\mathbf{a}]^-$ ($6 \times 10.3 = 62\%$ versus $6 \times 11.0 = 66\%$). Charge and spin then undergo an intermediate separation at $C\alpha$ and $C\gamma$, respectively ($6 \times 6.0 = 36\%$). Finally, the resonance form with adjacent spin and charge occurs with a low, but nonzero, weight in $[3\mathbf{a}]^-$ ($3 \times 0.7 = 2\%$). This resonance weighting is in qualitative accordance with calculated AIM spin densities: AIM($C\alpha$) = 48% (ELF resonance: 62%), AIM($C\beta$) = 9% (ELF resonance: 2%), AIM($C\gamma=C\delta$) = $2 \times 18 = 36\%$ (ELF resonance: 36%).^[36]

The number of a priori possible resonance forms increases with both reduction of symmetry and the extent of conjugation (substituted species $[n\mathbf{b}]^q$ were not considered). This number increases with charge as well. For the large dianion $[3\mathbf{a}]^{2-}$, for which monosynaptic valence basins (lone pairs) appear at the $C\alpha$ termini (Figure 3), the procedure led to three kinds of resonance forms (Figure 5). Two of them exhibit a $+/-$ charge separation, and the minus charge is clearly (de)localized at the $(C\gamma)_2C\beta=C\alpha$ corners with a strong weight at the $C\alpha$ termini.

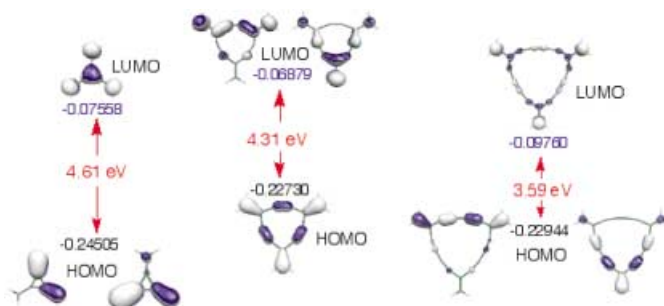


Figure 5. Frontier orbitals of neutral species $1\mathbf{a}$, $2\mathbf{a}$, and $3\mathbf{a}$.

In Figure 4 the formal numbers, n , of paired π_z electrons inside the ring are listed. They are calculated by using the weights (w_i) of the resonance form and the corresponding numbers n_i of paired π_z electrons inside the ring: $n = \sum w_i n_i$. Their utility is illustrated in the next section.

Proposition of an heuristic density-based Hückel-like rule: The unidimensional correlation of NICS versus $\sigma(d)$ (Figure 1)

works perfectly in the series $[1\mathbf{x}]^q$ and $[3\mathbf{x}]^q$, but fails for the series $[2\mathbf{x}]^-$ ($\mathbf{x} = \mathbf{a}, \mathbf{b}$). Beside $\sigma(d)$, other variables should therefore intervene in an eventual general correlation encompassing all the species. Considering that electron-density-based theoretical tools (AIM, ELF, ...) are modern alternatives to orbital-based tools, a formal continuous Hückel rule might be *heuristically* derived from electron density. According to the discrete *orbital*-derived Hückel rule, the aromatic character (e.g. the sign of the NICS) of annulenes depends on two variables: the singlet/triplet spin state ($S = 0, 1$) and the *parity* number of endocyclic paired π_z electrons ($n = 4m + 2, 4m$). Analogous rules were proposed for radialenes by Aihara.^[37b] In terms of *electron density*, n can be fractional (see preceding section) and its generalized “parity” could be expressed by a periodic function of n . We therefore sought for a correlation of the form:

$$\text{NICS} = A + B \sigma(d) + CF_S(n) \quad (2)$$

Here A , B , and C are constants, and $F(S, n)$ is a parity function of spin and electron numbers. Assuming a parity function form:

$$F_S(n) = [f_S \cos(n\pi/4) + (1 - f_S) \sin(n\pi/4)] \cos(n\pi/4)$$

and

$$f_S = \sin^2(S\pi)$$

we incidentally found that Equation (2) affords an excellent correlation for $A = -37.5$, $B = 410 \text{ \AA}^{-1}$, $C = 9.6$ ($R = 0.992$ for seven species: $[n\mathbf{a}]^q$, $q = 0, -1$, and $[3\mathbf{a}]^{2-}$).^[38]

This correlation is absolutely *not* theoretically demonstrated and limited to the above set of species. At this point, it is to be considered an empirical observation.

Orbital analysis: Hückel molecular orbital analysis of radialenes has long been derived. It has been used to calculate resonance energies, and a $4N/4N+2$ Hückel-type rule was proposed for even radialenes, where N is the (even) number of vinylidene units.^[37b] In contrast to their isomers benzene and carbobenzene, [3]radialene $1\mathbf{a}$ and carbo-[3]radialenes $2\mathbf{a}$, $3\mathbf{a}$ are nonalternate polyenes.^[39] Thus, according to a β -variable-Hückel treatment, [3]radialene exhibits doubly degenerate π MOs except for the lowest π -bonding MO and the LUMO. This is confirmed here with the DFT MOs (Figure 5). For expanded radialenes, the π MOs can be separated into π_z and π_{xy} types. In all cases, the HOMO and LUMO are of the π_z type. The π_z orbitals of $1\mathbf{a}$, $2\mathbf{a}$, $3\mathbf{a}$ are depicted in Figure 5. Whereas $3\mathbf{a}$ displays the same HOMO–LUMO degeneracy pattern as $1\mathbf{a}$, $2\mathbf{a}$ displays a converse pattern. This point is to be related to the peculiar behavior of the expanded series 2 with respect to series 1 and 3 , for the variation of NICS versus $\sigma(d)$.

As expected from consideration of the extension of the conjugation domain, the HOMO–LUMO gap is larger for the nonexpanded species $1\mathbf{a}$ (4.61 eV). It is however, larger by 0.72 eV for the singly expanded radialene $2\mathbf{a}$ than for the doubly expanded radialene $3\mathbf{a}$. Moreover both the HOMO

and LUMO of **2a** are, respectively, higher in energy than the HOMOs and LUMOs of both **1a** and **3a**. In other words **1a** and **3a** are less “reactive” than **2a**. This is a signature of a higher “chemical aromaticity” of **1a** and **3a** than with **2a**. It is well known that ground-state DFT MO eigenvalues are not meaningful as absolute electron energies, but are generally linearly correlated with the corresponding Hartree–Fock MO levels.^[40a] This has been verified for the neutral species **1a**, **2a**, and **3a**.^[40b] At the HF/6-31G** level, the value HOMO(**1a**) = −9.00 eV is in perfect agreement with the reported ionization potential $IE(\mathbf{1a}) = 9.0$ eV.^[41, 42] The HF HOMO–LUMO gap of **1a** (10.62 eV) is different from the energy gap ($\Delta E = 4.29$ eV) corresponding to the experimental UV/Vis absorption at $\lambda_{\max}(\mathbf{1a}) = 289$ nm.^[42] The HF two-level approximation is therefore not valid, but incidentally, it might be worth noting that the ΔE value is in agreement with the DFT HOMO–LUMO gap of **1a** (4.61 eV, Figure 5).

Electron affinities: In a first approach, the electron affinity, EA, can be estimated from the above MO diagram from the LUMO energy (Figure 5). Exact vertical and adiabatic EAs have also been calculated. The results listed in Table 3 show that the three EA measures are strongly correlated. The EAs increase as a function of the degree of *peripheral* expansion

Table 3. Electron affinity (B3PW91/6-31G** [eV]) versus the expansion degree of [3]radialene.^[a]

EA	1a	1b	2a	2b	3a	3b	[3a] [−]	[3b] [−]
− ϵ (LUMO)	2.08	3.49	1.89	3.02	2.67	3.51	−1.56	0.41
Vertical	0.07	2.05	0.33	1.72	1.22	2.45	−2.46	−0.62
Adiabatic	0.19	2.14	0.42	1.84	1.35	2.51	−2.40	−0.58

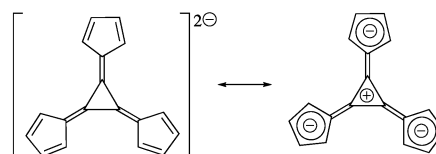
[a] The three measures are correlated by: Adiabatic EA \approx Vertical EA + 0.09 \approx − ϵ (LUMO) − 1.26 eV.

($EA([\mathbf{na}]^q) < EA([\mathbf{nb}]^q)$), but do not vary systematically as a function of the degree of *ring* expansion ($EA(\mathbf{2x}) < EA(\mathbf{1x}) < EA(\mathbf{3x})$, $x = \mathbf{a}, \mathbf{b}$). Nevertheless, the maximum EA value occurs for the doubly ring-expanded representatives **3**. These trends parallel the variation of aromaticity with monoelectronic reduction and ring expansion (Tables 1 and 2).

Regarding the second electron affinity, a weak but positive electron affinity of [**3a**][−] was anticipated from the weak enhancement of both magnetic and structural aromaticity in [**3a**]^{2−} (Table 1). Nonetheless, and despite the existence of three types of major resonance forms exhibiting 14 paired π_z electrons in [**3a**]^{2−}, the electron affinity of [**3a**][−] turns out to be even negative. This observation is finally in accordance with the localization of the last added electron of [**3a**]^{2−} in exocyclic monosynaptic ELF valence basins (lone pairs, see Figure 3).

Substitution of [**3a**]^{2−} by six ethynyl units results in an increase of the electron affinity by 1.8 eV in [**3b**]^{2−}. This observation is parallel to the enhanced structural–magnetic aromaticity of [**3b**]^{2−} as compared with [**3a**]^{2−} (Table 2). Although aromaticity (cyclic component of electron delocalization) is moderately affected by ethynyl substitution, the

external triple bonds here exert a strong (acyclic) delocalization effect. This observation is to be compared with the stabilization of the dianionic [3]radialene framework by delocalization toward three fulvene or 9-fluorenylidene substituents (Scheme 4).^[43] This stabilization is driven by the



Scheme 4. Aromaticity-stabilized [3]radialene dianion.

aromaticity of both the central cyclopropenium ring and of the three radial cyclopentadienyl anions. A similar argument accounted for the stability of the Fukunaga-type dianionic synthetic intermediate of hexaaryl[3]radialenes, and for the rather weakly negative second reduction potential of the latter as determined by cyclic voltammetry.^[22a]

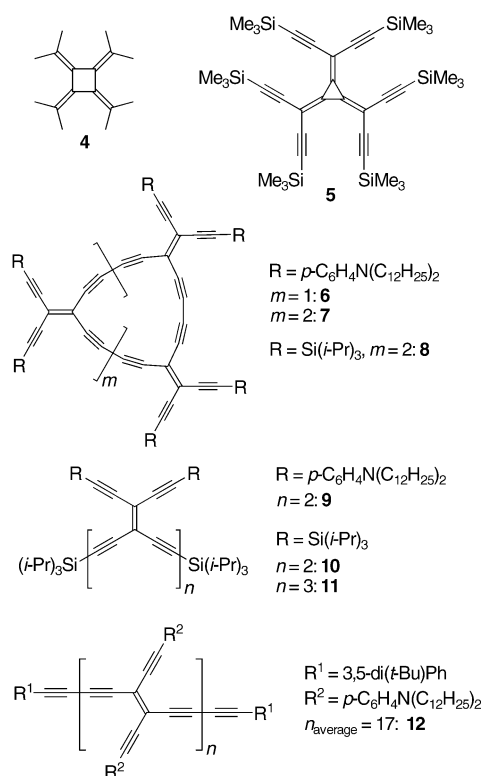
Although reduction potentials are not available for the parent compounds **1a,b**, **2a,b**, and **3a,b**, experimental studies have been performed on derivatives of **1a,b** and **3b**, while the carbo-[3]radialenes **2a,b** and **3a** are still elusive compounds that await to be synthesized. Yet, Tykwinski and co-workers^[44] have prepared a higher analogue of **2a**, an expanded [6]radialene, although no electrochemistry data are reported. Radialenes with the core of **3b** have been successfully synthesized from suitable tetraethynylethene (TEE) precursors.^[4b–e] However, attempts to synthesize derivatives of radialenes **3a** containing peripheral cyclohexylidene substituents by cyclization of related dendralenes have so far failed.^[44] It seems that the peripheral acetylene moieties in **3b** add a remarkable stability to these scaffolds. To our knowledge, the redox chemistry of [3]radialene **1a** or methylated derivatives thereof has never been exploited, whereas the octamethyl[4]-radialene **4** (Scheme 5) was subjected to an electrochemical study by Bock and Rohn (Table 4).^[45] This radialene was

Table 4. Cyclic voltammetry data for related species (see Scheme 5).^[a]

	4 ^[b]	5 ^[c]	6 ^[d]	7 ^[d]	8 ^[c]	9 ^[d]	10 ^[c]	11 ^[c]	12 ^[d]
E_{red}^1 [V]	−2.6	−0.96	−1.30	−1.28	−1.08	−1.63	−1.52	−1.36	−1.30
		(1e [−])	(1e [−])	(1e [−])	(1e [−])	(1e [−])	(1e [−])	(1e [−])	
E_{red}^2 [V]		−1.51	−1.60	−1.46	−1.28	−	−1.89	−1.74	−
		(1e [−])	(1e [−])	(1e [−])	(1e [−])		(1e [−])	(1e [−])	

[a] First and second reduction potentials are expressed versus Fc/Fc⁺ if not otherwise stated. [b] Solvent: DMF; potential versus SCE. [c] Solvent: THF. [d] Solvent: CH₂Cl₂.^[4b–e, 11, 45]

reduced at the very low potential of −2.6 V versus SCE in DMF, this corresponds roughly to about −3.0 V versus Fc/Fc⁺, hence at a considerably lower potential than that obtained for the perethynylated [3]radialene **5** (−0.96 V versus Fc/Fc⁺ in THF),^[11] a silylated derivative of **1b**.



Scheme 5. Experimentally known [4]- and [3]radialenes **4** and **5**, expanded [3]- and [4]radialenes **6–8**, and expanded dendralenes **9–11** and poly(triacetylene) **12** related to the theoretical species **1a**, **1b**, and **3b**, respectively.

However, care must be taken when extrapolating the influence of the peripheral acetylene groups by comparing radialenes of different ring sizes. Indeed, since the ionization energy of **1a** (IE = 9.0 eV,^[41] 8.94 eV^[42]) is significantly higher than that of **4** (IE = 7.30 eV^[45]), and the difference in the longest wavelength absorption maxima, reflecting the HOMO–LUMO gaps, only corresponds to about 0.3 eV (λ_{max} (**1a**) = 289 nm,^[42] λ_{max} (**4**) = 307 nm^[46]), then [3]radialene **1a** is expected to be more readily reduced than [4]radialene **4**, that is, at an anodically shifted potential and hence closer to that of **5**. The different substituents of **4** as compared with **1a** as well as the larger core size are important differences to take into account.

The electron-accepting strength of doubly expanded [3]- and [4]radialenes is very similar, that is, strong in both cases, as revealed by comparing **6** and **7**, both containing electron-donating anilino substituents.^[4d,e] Actually, the reductions occur slightly more readily for **7** than for **6**, in particularly the second reduction. These two radialenes differ by four paired π_z electrons inside the ring, and these rings are presumably planar in both cases. In contrast, we have found by X-ray crystallographic analysis that a doubly expanded [6]radialene adopts a nonplanar, chair-like conformation and is reduced at slightly more negative potential.^[4e] The enhanced electron affinity of perethynylated doubly expanded radialenes relative to their acyclic dendralene counterparts is evident when comparing the first and second reduction potentials between radialenes **6, 7** and TEE dimer **9**, and between radialene **8** and TEE dendralenes **10, 11**. The radialenes accommodate one or

two electrons much more readily. The strength of cyclic cross-conjugation is also revealed when noticing that radialenes **6** and **7** are even better electron acceptors than the linearly conjugated poly(triacetylene) **12**, which contains the same number of anilino moieties per TEE unit.^[4d]

The present calculations explain confidently, for the first time, the strong electron affinity of the perethynylated [3]radialenes **5** and **6** (and indirectly of the 17 π_z prearomatic [7][−] and [8][−]) by two factors: i) aromaticity enhancements when proceeding from the neutral core to the singly charged one and subsequently to the doubly charged one, ii) an acyclic delocalization effect exhibited by the external triple bonds. The NICS calculations showed that these two effects are not independent: ethynyl substitution enhances cyclic delocalization ([**3a**]^q versus [**3b**]^q, $q = 0, -1, -2$). Taking the calculational and experimental results together, it seems reasonable to make a generalization of the simple (integral) Hückel rule, allowing us to classify $4m+2 \pi_z$ structures of the type $[\text{C-H}]_6[\text{C-C}]_3^k\text{carbo-}[3]\text{radialene}(-2)$ ($k = 0, 2$) as aromatic: $k = 0$ implies $m = 0$ ($2\pi_z$), $k = 2$ implies $m = 3$ ($14\pi_z$), as well as structures of the type $[\text{C-H}]_8[\text{C-C}]_4\text{carbo-}[4]\text{radialene}(-2)$ ($m = 4, 18\pi_z$).

Conclusion

Both the theoretical tools used (ELF analysis,^[13, 31, 32] aromaticity theory,^[12] resonance theory^[34]), and the experimental targets studied (carbon-rich molecules,^[47] organic redox chemistry, organic chromophores) stand at the crossing point of active research domains. A concise summary of the results is that the question of the “aromaticity” of radialenes and their expanded versions is relevant but not univocal. The structural and magnetic criteria vary in a parallel manner. This variation can be analyzed in terms of cyclic electron delocalization from the electron density by using the ELF theory. The analysis is refined by using an heuristic density-based generalization of the orbital-based Hückel rule. Aromaticity (cyclic electron delocalization^[12]) gain is a driving force of facile reduction processes, measured by high electron affinities. Radial electron delocalization over ethynyl substituents, however, plays a determining role for the very strong magnetic aromatization of the antiaromatic anion [**2a**][−], and for the general enhancement of the electron affinity of monoanions. The energetic aromaticity criterion measured by d_{av} is orthogonal to structural and magnetic criteria. A refined measure of the former criterion (energetic effect of the cyclic component of delocalization, measured by resonance energies or aromatic stabilization energies) will require a comparison of expanded [3]radialenes with expanded dendralenes as acyclic references.^[48] The study of expanded [3]dendralenes is therefore the first natural prospect of this work.

As emphasized in the introduction, the parent [3]radialene framework was selected as a prototype, and we must remain aware that the results are quite homogeneously, but systematically, marked by the extreme steric strain of the ring size. On the other hand, the parent [6]radialene framework would correspond to the steric-strain-free situation (in the absence of cumbersome ethynyl substituents^[4e]). Such a study surely

deserves to be undertaken. Finally, it is worth noting that reduced cyclohexabutatrienylidene derivatives have recently been described.^[49] Following our above discussion, the expansion of [3]radialenes at the level of the exocyclic C=C bonds, leading to [C=C]₃carbo-[3]radialene(*q*) structures, appears a natural progression from both a theoretical and an experimental point of view.

The present calculations confidently support our previous hypothesis regarding the exceptional ability of doubly expanded [3]- and [4]radialenes to accommodate electrons, namely that this ability is promoted by aromaticity enhancements.

Acknowledgement

Financial support of this work by the CNRS is acknowledged. The authors wish to thank CALMIP (Calcul Intensif en Midi-Pyrénées, CICT, Toulouse) and IDRIS (Institut du Développement et des Ressources en Informatique Scientifique, Orsay, France) for computing facilities and Professor Bernard Silvi for fruitful discussions. R.C. also wishes to thank the French “Ministère de l’Enseignement Supérieur de la Recherche et de la Technologie” for additional support through ACI funding.

MBN thanks the Danish Technical Research Council for support.

- [1] a) H. Hopf, G. Maas, *Angew. Chem.* **1992**, *104*, 953; *Angew. Chem. Int. Ed. Engl.* **1992**, *31*, 931–954; b) *The Chemistry of Dienes and Polyenes, Vol. 1* (Ed.: Z. Rappoport, Series Eds.: S. Patai, Z. Rappoport), Wiley, Chichester, **1997**, pp. 927–977.
- [2] For peripheral expansion, see, for example: a) R. Diercks, J. C. Armstrong, R. Boese, K. P. C. Vollhardt, *Angew. Chem.* **1986**, *98*, 270; *Angew. Chem. Int. Ed. Engl.* **1986**, *25*, 268–269; b) U. H. F. Bunz, V. Enkelmann, *Organometallics* **1994**, *13*, 3823–3833; c) N. Jux, K. Holzer, Y. Rubin, *Angew. Chem.* **1996**, *108*, 2116; *Angew. Chem. Int. Ed. Engl.* **1996**, *35*, 1986–1990; d) U. H. F. Bunz, Y. Rubin, Y. Tobe, *Chem. Soc. Rev.* **1999**, *28*, 107–119.
- [3] For ring expansion, see for example: a) Y. Kuwatani, N. Watanabe, I. Ueda, *Tetrahedron Lett.* **1995**, *36*, 119–122; b) R. Chauvin, *Tetrahedron Lett.* **1995**, *36*, 401–404; c) R. Suzuki, H. Tsukuda, N. Watanabe, Y. Kuwatani, I. Ueda, *Tetrahedron* **1998**, *54*, 2477–2496; d) L. Maurette, C. Sui-Seng, M. Soleilhavoup, R. Chauvin in L. Maurette, Ph.D. Thesis, Université Paul Sabatier, Toulouse (France), **2002**.
- [4] a) H. Hopf, *Angew. Chem.* **1984**, *96*, 947; *Angew. Chem. Int. Ed. Engl.* **1984**, *23*, 948–960; b) A. M. Boldi, F. Diederich, *Angew. Chem.* **1994**, *106*, 480; *Angew. Chem. Int. Ed. Engl.* **1994**, *33*, 468–471; c) J. Anthony, A. M. Boldi, C. Boudon, J.-P. Gisselbrecht, M. Gross, P. Seiler, C. B. Knobler, F. Diederich, *Helv. Chim. Acta* **1995**, *78*, 797–817; d) M. Schreiber, R. R. Tykwinski, F. Diederich, R. Spreiter, U. Gubler, C. Bosshard, I. Poberaj, P. Günter, C. Boudon, J.-P. Gisselbrecht, M. Gross, U. Jonas, H. Ringsdorf, *Adv. Mater.* **1997**, *9*, 339–343; e) M. B. Nielsen, M. Schreiber, Y. G. Baek, P. Seiler, S. Lecomte, C. Boudon, R. R. Tykwinski, J.-P. Gisselbrecht, V. Gramlich, P. J. Skinner, C. Bosshard, P. Günter, M. Gross, F. Diederich, *Chem. Eur. J.* **2001**, *7*, 3263–3280; f) S. Eisler, R. R. Tykwinski, *Angew. Chem.* **1999**, *111*, 2138–2141; *Angew. Chem. Int. Ed.* **1999**, *38*, 1940–1943.
- [5] The “carbomeric” structures preserve the connectivity and symmetry of the parent Dreiding model and the resonance of the parent Lewis structure: R. Chauvin, *Tetrahedron Lett.* **1995**, *36*, 397–400.
- [6] See, for example: a) L. T. Scott, G. J. DeCicco, J. L. Hyun, G. Reinhardt, *J. Am. Chem. Soc.* **1983**, *105*, 7760–7761; b) L. T. Scott, G. J. DeCicco, J. L. Hyun, G. Reinhardt, *J. Am. Chem. Soc.* **1985**, *107*, 6546–6555; c) K. N. Houk, L. T. Scott, N. G. Rondan, D. C. Spellmeyer, G. Reinhardt, J. L. Hyun, G. J. DeCicco, R. Weiss, M. H. M. Chen, L. S. Bass, J. Clardy, F. S. Jorgensen, T. A. Eaton, V. Sarkozi, C. M. Petit, L. Ng, K. D. Jordan, *J. Am. Chem. Soc.* **1985**, *107*, 6556–6562; d) M. J. S. Dewar, M. K. Holloway, *J. Chem. Soc. Chem. Commun.* **1984**, 1188–1191; e) L. Maurette, C. Godard, S. Frau, C. Lepetit, M. Soleilhavoup, R. Chauvin, *Chem. Eur. J.* **2001**, *7*, 1165–1170; f) B. Leibrock, O. Vostrowsky, A. Hirsch, *Eur. J. Org. Chem.* **2001**, 4401–4409; g) A. de Meijere, S. I. Kozhushkov, *Chem. Eur. J.* **2002**, *8*, 3195–3202.
- [7] a) M. J. S. Dewar, M. K. Holloway, *J. Chem. Soc. Chem. Commun.* **1984**, 1188–1191; b) L. J. Schaad, B. A. Hess, Jr., L. T. Scott, *J. Phys. Org. Chem.* **1993**, *6*, 316–318; c) H. Jiao, N. R. J. v. E. Hommes, P. v. R. Schleyer, A. de Meijere, *J. Org. Chem.* **1996**, *61*, 2826–2828; d) C. Lepetit, B. Silvi, R. Chauvin, *J. Phys. Chem. A* **2003**, *107*, 464–473.
- [8] a) I. Yavari, A. Jabbari, M. Samadzadeh, *J. Chem. Res. Synop.* **1999**, 152–153; b) C. Godard, C. Lepetit, R. Chauvin, *Chem. Commun.* **2000**, 1833–1834; c) C. Lepetit, C. Godard, R. Chauvin, *New J. Chem.* **2001**, *25*, 572–580; d) J.-M. Ducere, C. Lepetit, P. G. Lacroix, J.-L. Heully, R. Chauvin, *Chem. Mater.* **2002**, *14*, 3332–3338.
- [9] E. A. Dorko, J. L. Hencher, S. H. Bauer, *Tetrahedron* **1968**, *24*, 2425–2431.
- [10] D. W. Rogers, F. J. McLafferty, *J. Phys. Chem. A* **2002**, *106*, 1054–1059.
- [11] T. Lange, V. Gramlich, W. Amrein, F. Diederich, M. Gross, C. Boudon, J.-P. Gisselbrecht, *Angew. Chem.* **1995**, *107*, 898; *Angew. Chem. Int. Ed. Engl.* **1995**, *34*, 805–809.
- [12] a) V. E. Minkin, M. N. Glukhovtsev, B. Y. A. Simkin, *Aromaticity and Antiaromaticity. Electronic and Structural Aspects*, Wiley, New York **1994**; b) T. M. Krygowski, M. K. Cyranski, Z. Czarnocki, G. Haferlinger, A. R. Katritzky, *Tetrahedron* **2000**, *56*, 1783–1796.
- [13] a) B. Silvi, A. Savin, *Nature* **1994**, *371*, 683–686; b) H. Chevreau, F. Fuster, B. Silvi, *Actual. Chim.* **2001**, *3*, 15–22.
- [14] For a recent discussion, see: L. Horný, N. D. K. Petraco, H. F. Schaeffer III, *J. Am. Chem. Soc.* **2002**, *124*, 14716–14720, and references therein.
- [15] Gaussian 98 (Revision A.7), M. J. Frisch, G. W. Trucks, H. B. Schlegel, G. E. Scuseria, M. A. Robb, J. R. Cheeseman, V. G. Zakrzewski, J. A. Montgomery, R. E. Stratmann, J. C. Burant, S. Dapprich, J. M. Millam, A. D. Daniels, K. N. Kudin, M. C. Strain, O. Farkas, J. Tomasi, V. Barone, M. Cossi, R. Cammi, B. Mennucci, C. Pomelli, C. Adamo, S. Clifford, J. Ochterski, G. A. Petersson, P. Y. Ayala, Q. Cui, K. Morokuma, D. K. Malick, A. D. Rabuck, K. Raghavachari, J. B. Foresman, J. Cioslowski, J. V. Ortiz, B. B. Stefanov, G. Liu, A. Liashenko, P. Piskorz, I. Komaromi, R. Gomperts, R. L. Martin, D. J. Fox, T. Keith, M. A. Al-Laham, C. Y. Peng, A. Nanayakkara, C. Gonzalez, M. Challacombe, P. M. W. Gill, B. G. Johnson, W. Chen, M. W. Wong, J. L. Andres, M. Head-Gordon, E. S. Replogle, J. A. Pople, Gaussian, Inc., Pittsburgh, PA, **1998**.
- [16] P. v. R. Schleyer, C. Maerker, A. Dransfeld, H. Jiao, N. J. R. v. E. Hommes, *J. Am. Chem. Soc.* **1996**, *118*, 6317–6318.
- [17] a) R. Ditchfield, *Mol. Phys.* **1974**, *27*, 789–807; b) K. Wolinski, J. F. Hinton, P. Pulay, *J. Am. Chem. Soc.* **1990**, *112*, 8251–8260; c) J. R. Cheeseman, G. W. Trucks, T. A. Keith, M. J. Frisch, *J. Chem. Phys.* **1996**, *104*, 5497–5509.
- [18] a) S. S. Shaik, P. C. Hiberty, J.-M. Lefour, G. Ohanessian, *J. Am. Chem. Soc.* **1987**, *109*, 363–374; b) Z. H. Yu, Z.-Q. Xuan, T.-X. Wang, H.-M. Yu, *J. Phys. Chem. A* **2000**, *104*, 1736–1747.
- [19] S. Noury, X. Krokidis, F. Fuster, B. Silvi, *TopMoD Package*, Université Pierre & Marie Curie, Paris, **1997**.
- [20] E. Pepke, J. Murray, J. Lyons, T.-Y. Hwu, *SciAn*, Supercomputer Research Institute of the Florida State University at Tallahassee, **1996**.
- [21] R. F. W. Bader, *Chem. Rev.* **1991**, *91*, 893–928.
- [22] a) T. Enomoto, N. Nishigaki, H. Kurata, T. Kawase, M. Oda, *Bull. Chem. Soc. Jpn.* **2000**, *73*, 2109–2114; b) M. Iyoda, N. Nakamura, M. Todaka, S. Ohtsu, K. Hara, Y. Kuwatani, M. Yoshida, H. Matsuyama, M. Sugita, H. Tachibana, H. Inoue, *Tetrahedron Lett.* **2000**, *41*, 7059–7064.
- [23] M. Diedenhofen, V. Jonas, G. Frenking, *J. Mol. Struct.* **2000**, *556*, 23–32.
- [24] T. M. Krygowski, M. Cyranski, *Chem. Rev.* **2001**, *101*, 1385–1420, and references therein: a) $GEO = \alpha^2(d)$. GEO is the geometric component of the structural aromaticity parameter (HOMA). b) $EN = \alpha(d_{av} - d_{opt})^2$, in which d_{opt} is the bond length in the most stable aromatic system and is estimated from the harmonic oscillator model. EN is the energetic component of the HOMA parameter. c) α is an empirical parameter and $HOMA = 1 - GEO - EN$.

- [25] I. Alkorta, I. Rozas, J. Elguero, *Tetrahedron* **2001**, *57*, 6043–6049.
- [26] a) D. Quinonero, A. Frontera, P. Ballester, P. M. Deya, *Tetrahedron Lett.* **2000**, *41*, 2001–2005; b) P. v. R. Schleyer, K. Najafian, B. Kiran, H. Jiao, *J. Org. Chem.* **2000**, *65*, 426–431; c) D. Quinonero, C. Garau, A. Frontera, P. Ballester, A. Costa, P. M. Deya, *Chem. Eur. J.* **2002**, *8*, 433–438.
- [27] M. K. Cyranski, T. M. Krygowski, *Tetrahedron* **1999**, *55*, 6205–6210.
- [28] The calculation of d_{opt} for annulenes and benzenoids requires a reference to “pure” C–C and C=C bond lengths. d_{opt} , however, depends on the “bond type” and, in the case of (C–C)^kcarbo-[3]radialenes, several d_{opt} values should be first determined for: CH₂=C, =C–C≡, ≡C–C≡, –C≡C–. This would here preclude a highly predictive value of the final ENs.
- [29] P. v. R. Schleyer, P. K. Freeman, H. Jiao, B. Goldfuss, *Angew. Chem.* **1995**, *107*, 332; *Angew. Chem. Int. Ed. Engl.* **1995**, *34*, 337–340.
- [30] a) A. R. Katritzky, P. Barczynski, G. Musumarra, D. Pisano, M. Szafran, *J. Am. Chem. Soc.* **1989**, *111*, 7–15; b) A. R. Katritzky, K. Jug, D. C. Oniciu, *Chem. Rev.* **2001**, *101*, 1421–1450.
- [31] a) A. Savin, B. Silvi, F. Colonna, *Can. J. Chem.* **1996**, *74*, 1088–1096; b) A. Savin, R. Nesper, S. Wengert, T. F. Fässler, *Angew. Chem.* **1997**, *109*, 1892–1918; *Angew. Chem. Int. Ed. Engl.* **1997**, *36*, 1809–1832; c) S. Noury, F. Colonna, A. Savin, B. Silvi, *J. Mol. Struct.* **1998**, *450*, 59–68; d) D. B. Chesnut, J. L. Bartolotti, *Chem. Phys.* **2000**, *253*, 1–11; d) D. B. Chesnut, L. J. Bartolotti, *Chem. Physics* **2000**, *257*, 175–181; f) R. Choukroun, B. Donnadiou, J.-S. Zhao, P. C. Cassoux, C. Lepetit, B. Silvi, *Organometallics* **2000**, *19*, 1901–1911; e) F. Fuster, B. Silvi, *Theor. Chem. Acc.* **2000**, *104*, 13–21.
- [32] U. Häussermann, S. Wengert, R. Nesper, *Angew. Chem. Int. Ed. Engl.* **1994**, *33*, 2073–2076; *Angew. Chem.* **1994**, *106*, 2150.
- [33] See for example: a) B. Pullman, *C. R. Acad. Sci.* **1946**, *222*, 1106–1107; b) J. E. Huheey, *Inorganic Chemistry*, 2nd ed., Harper, N.Y., **1978**, p. 111; c) W. Schubert, W. Ellenrieder, *J. Chem. Res. Synop.* **1984**, 256–257.
- [34] See for example: W. L. Jolly, W. B. Perry, *J. Am. Chem. Soc.* **1973**, *95*, 5442–5450; b) W. L. Jolly, W. B. Perry, *Inorg. Chem.* **1974**, *13*, 2686–2692; c) P. C. Hiberty, G. Ohanessian, *Int. J. Quantum Chem.* **1985**, *27*, 259–272; d) C. L. Perrin, *J. Am. Chem. Soc.* **1991**, *113*, 2865–2868; e) E. D. Glendening, J. A. Hrabal II, *J. Am. Chem. Soc.* **1997**, *119*, 12940–12946; f) E. D. Glendening, F. Weinhold, *J. Comput. Chem.* **1998**, *19*, 593–609; g) V. Bachler, N. Metzler-Nolte, *Eur. J. Inorg. Chem.* **1998**, 733–744; h) V. Bachler, K. Schaffner, *Chem. Eur. J.* **2000**, *6*, 959–970; i) I. S. Han, C. K. Kim, C. K. Kim, H. W. Lee, I. Lee, *J. Phys. Chem. A* **2002**, *106*, 2554–2560.
- [35] The equations were written down after averaging the basin populations of identical chemical type and assuming a *pseudo-D*_{3h} symmetry. Rigorous analysis in the actual C_{2v} symmetry does not improve the resolution of the equation system.
- [36] While ELF resonance weighting assigns the whole 36% spin density at C γ and no spin density at C δ , AIM shares this density equally between C γ and C δ (2 × 18%). The ELF–AIM accordance thus merely refers to the C δ ≡C γ bond.
- [37] a) B. A. Hess, Jr., L. J. Schaad, *J. Am. Chem. Soc.* **1971**, *93*, 305–310; b) J.-i. Aihara, *Bull. Chem. Soc. Jpn.* **1975**, *48*, 517–520; c) J.-i. Aihara, *Bull. Chem. Soc. Jpn.* **1980**, *53*, 1751–1752.
- [38] For hexaethynyl species [nb]^q, n is not efficiently calculated due to the high number of possible resonance forms. Nevertheless, as soon as [na]^q and [nb]^q have similar NICS values (this is not the case for [2a]⁻ and [2b]⁻: NICS([2a]⁻) = +4 ppm ≫ NICS([2b]⁻) = -16.4 ppm), we may assume that n([nb]^q) ≈ n([na]^q). Under this assumption, we obtain a smooth correlation, which now extends over 13 species. This shows that whereas NICS sometimes varies rapidly with n, σ (d) always varies smoothly with n (see Supporting Information).
- [39] N. Tyutyulkov, F. Dietz, K. Müllen, M. Baumgarten, S. Karabunarliev, *Chem. Phys.* **1994**, *189*, 83–97.
- [40] a) R. Stowasser, R. Hoffmann, *J. Am. Chem. Soc.* **1999**, *121*, 3414–3420; b) For occupied π_z MOs, the correlations read: $E_k(\text{DFT}) = 0.016 + 0.79 E_k(\text{HF})$ for **1a** (2 points) and $E_k(\text{DFT}) \approx 0.75 E_k(\text{HF})$ for **2a**, **3a**. The average slope (≈ 0.76) is slightly larger than that operating for carbo-[N]annulenes (0.61 for all π_z MOs, 0.63 for occupied π_z MOs only; see ref. [8c]).
- [41] E. A. Dorko, R. Scheps, S. A. Rice, *J. Phys. Chem.* **1974**, *78*, 568–571.
- [42] T. Bally, E. Haselbach, *Helv. Chim. Acta* **1978**, *61*, 754–761.
- [43] M. Iyoda, H. Kurata, M. Oda, C. Okubo, K. Nishimoto, *Angew. Chem.* **1993**, *105*, 97; *Angew. Chem. Int. Ed. Engl.* **1993**, *32*, 89–90.
- [44] E. Burri, F. Diederich, M. B. Nielsen, *Helv. Chim. Acta* **2002**, *85*, 2169–2182.
- [45] H. Bock, G. Rohn, *Helv. Chim. Acta* **1991**, *74*, 1221–1232.
- [46] M. Iyoda, S. Tanaka, H. Otani, M. Nose, M. Oda, *J. Am. Chem. Soc.* **1998**, *110*, 8494–8500.
- [47] a) A. de Meijere (vol. Ed.), *Top. Curr. Chem.* **1998**, *196*, whole issue; b) A. de Meijere (vol. Ed.), *Top. Curr. Chem.* **1999**, *201*, whole issue.
- [48] Y. Zhao, K. Campbell, R. R. Tykwinski, *J. Org. Chem.* **2002**, *67*, 336–344.
- [49] S. Ito, H. Inabe, N. Morita, K. Ohta, T. Kitamura, K. Imafuku, *J. Am. Chem. Soc.* **2003**, *125*, 1669–1680.

Received: April 24, 2003 [F5070]